



Non-linear Holocene climate evolution in the North Atlantic: a high-resolution, multi-proxy record of glacier activity and environmental change from Hvítárvatn, central Iceland

Darren J. Larsen^{a,b,*}, Gifford H. Miller^{a,b}, Áslaug Geirsdóttir^b, Sædís Ólafsdóttir^b

^a Department of Geological Sciences, INSTAAR, University of Colorado, UCB 450, Boulder, CO 80309, USA

^b Institute of Earth Sciences, University of Iceland, Sturlugata 7, Reykjavík 101, Iceland

ARTICLE INFO

Article history:

Received 6 October 2011

Received in revised form

8 February 2012

Accepted 10 February 2012

Available online 17 March 2012

Keywords:

Iceland

Lake sediment

Glacier erosion

Soil erosion

Holocene paleoclimate

8.2 Event

Holocene thermal maximum

Neoglaciation

Medieval warm period

Little Ice Age

ABSTRACT

Iceland is well situated to monitor North Atlantic Holocene climate variability. Terrestrial sites there offer the potential for well-dated, high-resolution, continuous records of environmental change and/or glacier activity. Laminated sediments from the proglacial lake Hvítárvatn provide a continuous record of environmental change and the development of the adjacent Langjökull ice cap for the past 10.2 ka. Replicate lake sediment cores, collected from multiple locations in the basin, are placed in a secure geochronology by splicing a varve chronology for the past 3 ka with a tephra-constrained, paleomagnetic secular variation derived chronology for older sediments. Multiple proxies, including sedimentation rate, bulk density, ice-rafted debris, sediment organic matter, biogenic silica, and diatom abundance, allow annual to multi-decadal resolution and reveal a dynamic Holocene terrestrial climate. Following regional deglaciation of the main Iceland Ice Sheet, summer temperatures were high enough that mountain ice caps had already melted, or were contributing insignificant sediment to the lake. Pronounced increases in sedimentation rate, sediment density, and the influx of terrestrial organic matter, between 8.7 and 7.9 ka suggest early Holocene warmth was interrupted by two distinct pulses of cold summers leading to widespread landscape destabilization and possibly glacier growth. The Holocene thermal maximum (HTM; 7.9 to 5.5 ka) was characterized by high within-lake productivity and ice-free conditions in the watershed. Neoglaciation is recorded as a non-linear transition toward cooler summers, landscape destabilization, and the inception and expansion of Langjökull beginning ca 5.5 ka, with notable increases in ice cap size and landscape instability at 4.2 and 3.0 ka. The past two millennia are characterized by the abrupt onset of sustained cold periods at ca 550 and 1250 AD, separated by an interval of relative warmth from ca 950 to 1150 AD. The greatest Holocene extent of Langjökull occurred in the nineteenth century and is coincident with peak landscape instability, followed by ice recession throughout the twentieth century.

© 2012 Elsevier Ltd. All rights reserved.

1. Introduction

The primary control on Northern Hemisphere climate during the Holocene has been the monotonic decline in Northern Hemisphere summer insolation, related to the precession of the equinoxes (Berger and Loutre, 1991). However, despite this nearly linear forcing, strong evidence exists for widespread and regionally correlative perturbations in Holocene climate that have been both periodic and abrupt in nature, and that have underscored the sensitivity of the climate system to additional forcings and

* Corresponding author. Department of Geological Sciences, INSTAAR, University of Colorado, UCB 450, Boulder, CO 80309, USA. Tel.: +1 303 492 7808.

E-mail address: darren.larsen@colorado.edu (D.J. Larsen).

feedbacks (e.g. Mayewski et al., 2004 and references therein). The non-linear nature of these centennial-scale changes reflects the disproportionate response of the climate system to a relatively constant factor. Associated with many of the perturbations is the role of North Atlantic Ocean circulation in global heat distribution, including the strength of the thermohaline circulation and the position of North Atlantic Deep Water (NADW) formation (e.g. Denton and Broecker, 2008; Sicre et al., 2008). Because variations in these marine systems are often preserved in sedimentary archives, investigations conducted in the North Atlantic have been successful in documenting Holocene paleoceanographic changes (e.g. Eiríksson et al., 2000a; Oppo et al., 2003; Bendle and Rosell-Melé, 2007; Massé et al., 2008; Ólafsdóttir et al., 2010). What remains unclear is how these oceanographic changes have been manifested

on land, or how nonlinearities in Holocene climate have been expressed in terrestrial environments.

Iceland ($\sim 103,000 \text{ km}^2$) is the largest landmass in the central North Atlantic and is positioned in a region with strong ocean and atmospheric thermal gradients (e.g. Knudsen and Eiríksson, 2002, Fig. 1a). Holocene climate in Iceland has been reconstructed from a variety of geologic records (e.g. Hallsdóttir, 1991, 1995; Gudmundsson, 1997; Rundgren, 1998; Stötter et al., 1999; Kirkbride and Dugmore, 2001, 2006; Wastl et al., 2001; Caseldine et al., 2003, 2006; Hallsdóttir and Caseldine, 2005; Wastl and Stötter, 2005; Hannesdóttir, 2006; Axford et al., 2007, 2009; Geirsdóttir et al., 2009a,b; Langdon et al., 2010) but remains coarsely resolved and largely incomplete or discontinuous. A recent review of Holocene glacier and climate fluctuations in Iceland highlights important issues that remain unresolved (Geirsdóttir et al., 2009b). What was the timing and character of early Holocene warmth in central Iceland, and was it sufficient to completely melt Iceland's ice caps? Did Iceland experience periodic or non-linear climate changes such as the 8.2 ka cold event? When was the onset of Neoglaciation and

what was the evolution of large ice caps through the mid to late Holocene? The goal of this paper is to directly address these questions using multiple physical, biological, and chemical proxies contained in sediments from an ideally positioned proglacial lake in Iceland's central highlands.

Lake basins preserve a record of environmental change by continuously accumulating sediment and climate proxies produced within the lake and from their surrounding catchments. In glacier-dominated catchments, where sedimentation rates are high and sediment deposition is influenced by upstream ice erosion and meltwater transport, lacustrine archives can also reflect the evolution of glacier activity in response to changes in regional climate and can be inspected at high-resolution (e.g. Desloges, 1994; Dahl et al., 2003; Larsen et al., 2011). This study exploits well-dated glacially derived sediments from Hvítárvatn, a glacial lake adjacent to Langjökull, second largest of Iceland's ice caps, to provide a continuous, high-resolution (annual to multi-decadal), multi-proxy record of Holocene environmental change and ice cap activity in Iceland.

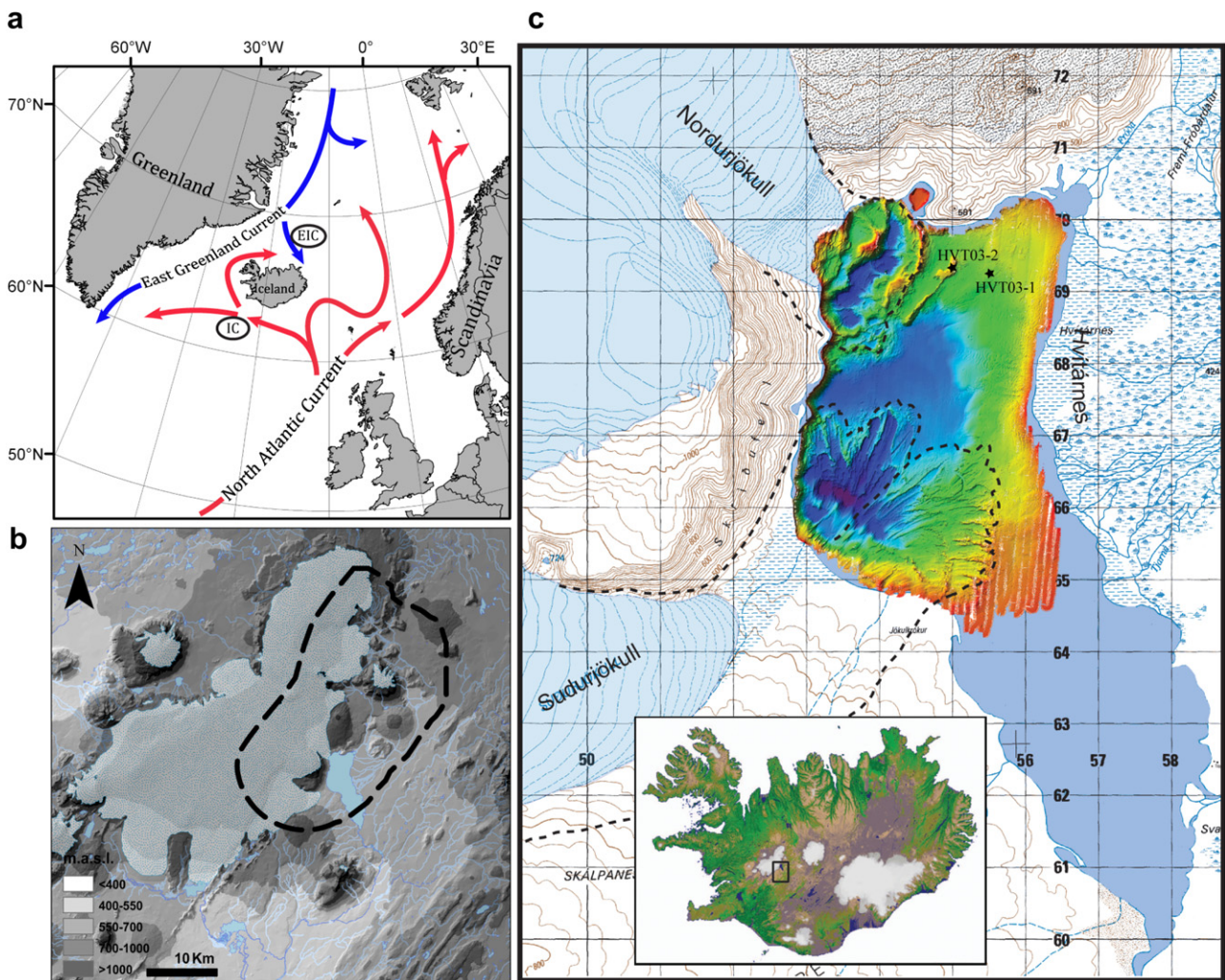


Fig. 1. (a) Map of Iceland in the North Atlantic showing generalized ocean current circulation. At present, Iceland is located near the boundary between contrasting water masses. The Irminger Current (IC), a branch of the warm and saline North Atlantic Current, bends around the south and west coasts, while the colder and fresher East Iceland Current (EIC) descends from the north with the East Greenland Current. (b) Location map and approximate catchment area (dashed line) of Hvítárvatn seen adjacent to the Langjökull ice cap. (c) Topographic map of field area (gridlines on map are 1 km^2) with inset map highlighting the position of the lake within Iceland. The current ice margins of the outlet glaciers Nordurjökull and Suðurjökull are shown along with their approximate LIA maximum limits (dashed lines). Bathymetric map illustrates water depth in the main basin (cooler colors reflect increasing depth) and the location of the two cores sites, HVT03-1 and HVT03-2. Image modified from Geirsdóttir et al. (2008). (For interpretation of the references to color in this figure legend, the reader is referred to the web version of this article.)

2. Study site

Hvítárvatn (64°37' N, 19°51' W; 422 m asl) is a glacially dominated lake situated along the eastern margin of Langjökull (925 km²), in the central Iceland highlands (Fig. 1b). The lake has a surface area of 28.9 km² (ca 10 × 3 km), a maximum depth of 83 m, and lies within an 820 km² catchment. Measurements of water temperature, pH, specific conductance, and dissolved oxygen demonstrate that Hvítárvatn is well mixed, with no significant thermal stratification in summer (Black, 2008). Mean annual temperature and precipitation recorded at Hveravellir (641 m asl), a town ~30 km north of the lake, are -0.9 °C and 730 mm, respectively (Iceland Meteorological Office; reference period: 1966–2003 AD). The ice-free season at Hvítárvatn commonly lasts six months (between May and October), although prolonged ice cover and/or early winter thaw may occur.

Presently, over one-third of the Hvítárvatn watershed is occupied by Langjökull, and glacially derived meltwater contributes ~72% of the total inflow to the lake (Flowers et al., 2007). High sedimentation rates, particularly during the past few centuries (~1 cm a⁻¹; Larsen et al., 2011), and a turbid water column, reflect the efficient production and delivery of glacially derived erosion products to the lake. Primary sediment sources are two outlet glaciers, Suðurjökull and Norðurjökull, and two meltwater streams that emanate north of the lake. Suðurjökull and Norðurjökull are warm-based glaciers that have catchments of ~61 and ~37 km², respectively (Palmer et al., 2009). Both glaciers advanced into Hvítárvatn during the Little Ice Age (LIA; Larsen et al., 2011), but have receded from their clearly defined LIA maxima, and no longer reach the lake (Fig. 1c; Geirsdóttir et al., 2008). Sediment transported by the other two meltwater streams has created the Hvítárnés delta, an expansive wetland area along the northeastern shore (Fig. 1b,c). Seismic profiles reveal thickening lacustrine sediment sequences towards this feature, suggesting active progradation of the delta during the late Holocene (Black et al., 2004). Lake drainage occurs to the southeast over a bedrock sill that is overlain by large boulder residuals. The outlet channel has an average monthly discharge of 45 m³ s⁻¹ (range: 23–94 m³ s⁻¹; reference period: 1961–1990 AD), contains an average suspended sediment load of 35 mg L⁻¹, and accounts for the removal of roughly half of the sediment delivered to the lake before it settles (Pálsson and Vigfússon, 1996). A seismic reflection survey reveals over 65 m of postglacial sediment in the main depositional basin (Black et al., 2004), and the presence of the Saksunarvatn tephra in the sediment fill confirms that the Iceland Ice Sheet had retreated from Hvítárvatn prior to 10.2 ka (Jóhannsdóttir, 2007). Multiple paleo-shorelines, reaching up to nearly 200 m above the present lake level, are preserved in the hillslopes on the north and west margins of the lake. These shorelines have been interpreted to represent multiple stages of an ice-dammed lake that formed in the basin during the retreat of the Iceland ice sheet from the region (Tómasson, 1993). There is no evidence for significant lake level changes after 10.2 ka.

3. Materials and methods

3.1. Sediment cores and physical proxies

Paired sediment cores were collected in an overlapping manner from four locations in Hvítárvatn using the DOSECC GLAD-200 core rig (<http://www.dosecc.org/>). This study focuses on two coring locations: HVT03-1 in the central northern flats, and HVT03-2 situated on a hyaloclastic ridge fronting the Norðurjökull terminal moraine (Larsen et al., 2011). At both sites, 3 m core drives were drilled in pairs with a 1.5 m offset to ensure continuous recovery.

Surface cores capture the sediment–water interface and undisturbed upper sediments, following the methodology outlined in Glew (1991). Total recovery of the spliced cores at the two individual coring locations exceeded 95%. Core sections were cut into 1.5 m lengths, packaged in the field, and shipped to the Limnological Research Center (LRC) at the University of Minnesota for initial core processing, description and sub-sampling.

The Hvítárvatn cores were analyzed for multiple physical and organic matter proxies directly related to ice cap activity and paleoenvironmental conditions. In glacier occupied basins, lake sediment physical characteristics, including density, magnetic susceptibility (MS), and grain size distribution, are primarily influenced by the contribution of glacially eroded material (e.g. Dahl et al., 2003 and references therein). Whole-core density and MS were measured in 1 cm intervals using the gamma-ray attenuation porosity evaluator (GRAPE) logging system. The Core segments were then split, and core halves were photographed using a DMT CoreScan Color flatbed scanner. Medical X-ray images of core halves were taken at the Wardenburg Health Center, University of Colorado, to better document sedimentary structures, including ice-rafted debris (IRD). Here, IRD is defined as clasts with a grain diameter ≥2 mm and was counted in 20-year intervals according to the age model developed for each core. The transport and deposition of IRD to the core sites is principally accomplished by iceberg rafting and is restricted to periods when either of the two outlet glaciers terminated in Hvítárvatn and maintained an active calving front (Larsen et al., 2011). IRD counts were performed on digitally scanned X-ray core images placed alongside respective Corescan images. Grain size analyses were conducted at 1–50 cm resolution using a Malvern Long Bed Mastersizer at the Institute of Arctic and Alpine Research (INSTAAR), University of Colorado.

3.2. Organic matter proxies

Sedimentary organic matter (OM) proxies are often used to evaluate changes in the source and production of vegetation growing in and around lake systems. Samples for total carbon (TC), stable carbon isotopes (δ¹³C), and total nitrogen (TN), were taken at 1–10 cm intervals from cores HVT03-1A/1B and HVT03-2A/2B/2C, and at 2.5 cm intervals from the surface core HVT03-1C. All samples were processed at the University of California, Davis using a PDZ Europa ANCA-GSL elemental analyzer interfaced with a PDZ Europa 20–20 isotope ratio mass spectrometer (IRMS). Freeze-dried samples were combusted at 1020 °C and nitrogen and CO₂ gas were separated on a Carbosieve GC column (65 °C, 65 mL/min) before entering the continuous-flow IRMS for δ¹³C measurements. δ¹³C values are expressed relative to Vienna Pee Dee Belemnite. Because the lake sediment is devoid of inorganic carbon, TC is derived exclusively from organic material and represents total organic carbon (TOC). Traditionally, TOC is used as a measure of within-lake primary productivity (Meyers and Teranes, 2001). However, in Iceland, where sedimentation rates are high and primary productivity is relatively low, TOC is strongly influenced by the influx of terrestrial OM and clastic material (Geirsdóttir et al., 2009a; Larsen et al., 2011). To compensate for highly variable sedimentation rates, TOC concentrations (TOC%) were converted to fluxes using: $TOC_Q = (TOC\%/100)\rho_B Z$, where the yearly flux of carbon (TOC_Q) is equal to the product of TOC%, bulk density (ρ_B) and sediment thickness (Z; determined from varve thickness data for the past 3 ka and PSV-derived average sedimentation rates for older sediments). This conversion facilitates the evaluation of the mass of sedimentary OM deposited at the lake independent of sedimentation rate.

The elemental mass ratio (C:N) of each sample was calculated to determine the relative proportions of terrestrial and aquatic OM in

the lake sediment. To provide constraints on the terrestrial end member of C:N and $\delta^{13}\text{C}$ of lake sediment OM, soil samples from multiple terrestrial stratigraphic sections excavated around Hvítárvatn were analyzed. These samples include sediment deposition spanning at least the last 6 ka, according to the regional tephrostratigraphy (Kirkbride and Dugmore, 2006 and references therein).

Diatom assemblages are commonly used bioindicators of paleoenvironmental conditions in lake habitats and were analyzed in core HVT03-1A at approximately 100-year resolution (Black, 2008). Identification and counting of diatoms was performed on an Olympus Vanox microscope using an oil immersion objective at 1000 \times magnification. More than 200 diatom valves were counted for each sample, although in many late Holocene intervals, where diatoms were scarce, approximately 100 valves per slide were counted. Diatom percentages were calculated from the total diatom sum, while total diatom concentration is shown as 10^7 valves g^{-1} sediment.

Biogenic Silica (BSi) is an amorphous form of silica that is biogenically precipitated in the water column by a variety of aquatic organisms. In lake sediments, it primarily encompasses diatom frustules (Conley and Schelske, 2002) and like diatom abundance, can be a reliable measure of primary productivity, if other variables (i.e. sedimentation rate and dissolution potential) are constrained. BSi was sampled in core HVT03-1 with at least one sample every 40 years, and decadal resolution for most of the last 3 ka, and measured at the University of Illinois, following methods outlined by Mortlock and Froelich (1989), except for the use of 10% Na_2CO_3 solution during extraction. A Spectronic Genesys 5 spectrophotometer was used to measure BSi concentration, which was then converted to weight percent SiO_2 of dry bulk sediment.

3.3. Chronology

Accurate age control of the sediment cores is obtained by splicing a varve chronology of the past 3 ka with a paleomagnetic secular variation (PSV) derived chronology for older sediments. Both chronologies are constrained by a robust tephrochronology spanning the past 10.2 ka (Jóhannsdóttir, 2007; Jagan, 2010). Hvítárvatn sediments have proved unsuitable for radiocarbon dating due to variable fluxes of aged terrestrial carbon reworked by ice and wind (Black, 2008).

3.3.1. Tephrochronology

The tephrostratigraphy around Hvítárvatn is well established from historical records after ca 900 AD, and from soil and lacustrine sequences for older eruptions (Kirkbride and Dugmore, 2006; Jóhannsdóttir, 2007; Jagan, 2010). Tephra horizons are useful for correlating between sediment cores and for absolute dating, and were detected visually and sub-sampled for chemical composition. Tephra preparation was performed according to the procedures outlined in Jóhannsdóttir (2007). Major element glass analyses were carried out on a Cameca SX100 energy dispersive electron microprobe at the NERC Tephra Analysis Unit at the University of Edinburgh and University of Hawaii at Manoa using a 5–8 μm beam size, 15 kV acceleration voltage, 2 nA beam-current at Edinburgh, and 15 kV acceleration voltage, 15 nA beam-current and $8 \times 12 \mu\text{m}$ rastered and defocused beam at Hawaii. The geochemical composition of multiple size fractions from each tephra layer was compared to the University of Edinburgh tephra glass chemistry database, and combined with stratigraphic information to identify source volcano and eruption (e.g. Jóhannsdóttir, 2007). Although over 100 tephra layers have been geochemically identified in the Hvítárvatn sediment archive (Jóhannsdóttir, 2007; Jagan, 2010), the primary Holocene tephrochronologies of cores HVT03-1 and HVT03-2 are constructed from ten primary tephra layers described in Larsen et al. (2011) and Ólafsdóttir (2010).

3.3.2. Varve chronology

The upper portion of each core is characterized by well-defined, alternating, olive black to light yellow laminations, composed of siliciclastic fine sand, silt and clay (Fig. 2a,b). Grain size analysis and tephrostratigraphy demonstrate that these laminated packages are produced annually, continuous in nature, and comprise glacially derived clastic varves (Larsen et al., 2011). A multiple core varve chronology was constructed for the past ca 3 ka by performing independent layer counts on three sediment cores, and correlating them to each other using distinct laminae, tephra and stratigraphic sequences (Larsen et al., 2011). Age uncertainty for the final varve chronology from the core top down to the Settlement tephra layer (871 ± 2 AD; Grönvold et al., 1995) is ± 6 years. Below this isochron, age uncertainty increases from ± 6 years at the Settlement Layer to approximately ± 100 years at the Hekla 3 tephra layer (H3; varve year 982 BC). The increased counting error in the earlier portion of the record results from periods of relatively low sedimentation rates (thinner, less defined varves) and the length of time (~ 1800 years) between control points. Varves have not been counted below H3, yet visual observations suggest that varves continue down-core to a depth below the Hekla 4 tephra (4260 ± 20 cal a BP; Dugmore et al., 1995) where they become indistinct. The lower portion of the sediment cores are dark gray to black in color, and are characterized by faint and irregular, non-annual laminations (Fig. 2c).

3.3.3. PSV chronology

PSV analyses of Hvítárvatn sediments were carried out by Ólafsdóttir (2010). Paleomagnetic measurements of U-channel samples from core HVT03-1 were conducted at 1 cm intervals at the University of Florida using a 2G Enterprise superconducting rock magnetometer. Patterns in the component declination and inclination records from the lake core were correlated to the PSV record of marine core MD99-2269 (Stoner et al., 2007) using the analyses software (Paillard et al., 1996). MD99-2269 is a 25-m-long marine sediment core from the north Iceland shelf that contains an age model based on 44 radiocarbon dates from two different synchronized cores (Stoner et al., 2007) and corrected for local marine reservoir age variability (Kristjánsdóttir et al., 2007). Age uncertainty for this core is primarily related to temporal changes in the marine reservoir age and is estimated to be 100–200 years. The MD99-2269 age model is projected onto the older Hvítárvatn sediments using diagnostic tephra horizons and 15 tie points to synchronize the marine and lake core PSV records in the depth domain (Ólafsdóttir, 2010).

4. Results and proxy interpretations

4.1. Chronology

The tephra-constrained varve- and PSV-derived chronologies are spliced together at the H3 tephra layer, resulting in a continuous age-depth model for core HVT03-1 that spans the past ca 10.2 ka (Fig. 3). Although chronologic control is high for the entirety of the record, error in the age model generally increases with age and length of time from nearest control point, from ± 10 years for the past millennium to a maximum of ± 100 –200 years for oldest sediments (Ólafsdóttir, 2010; Larsen et al., 2011).

4.2. Physical properties

Physical proxies exhibit both millennial-scale trends and multi-decadal to centennial excursions (Fig. 4). When glacial ice occupies a lake watershed, the production and delivery of sediment is dominated by subglacial erosion and meltwater discharge (e.g. Karlén, 1981). At Hvítárvatn, on multi-decadal and longer

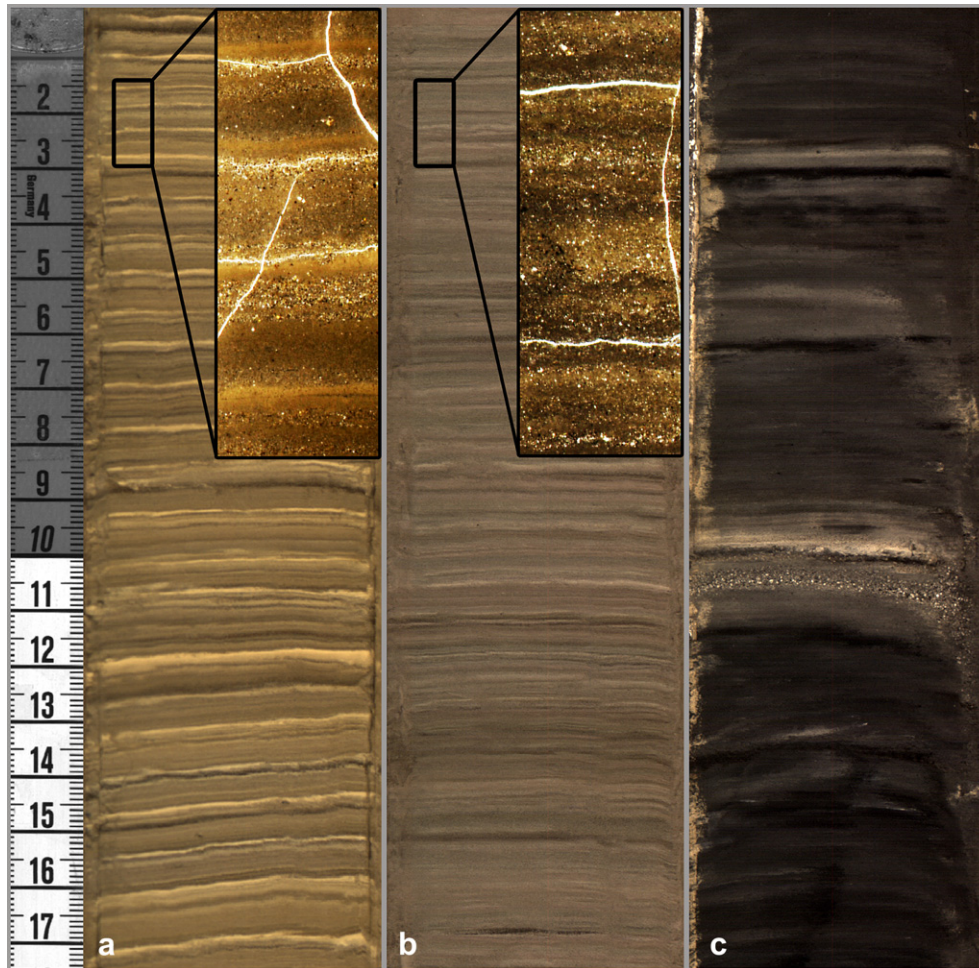


Fig. 2. Images (flatbed scans with insets of enlarged thin sections) of lake sediments from different depths in core HVT03-1. The uppermost sediments (a) display clastic varved structure, with thicker laminations characterizing the centuries of the Little Ice Age (Larsen et al., 2011). Varve thickness is decreased at a depth of 7.5 m (b) corresponding to the Neoglacial period. The lower portion of the core (c) contains faint and irregular laminations, not interpreted to be varves. Note the position of the Hekla 5 tephra layer (~7050 cal a BP) at ~10 cm depth in (c).

timescales, we interpret both processes to be a function of ice cap size, which varies according to long-term trends in Langjökull mass balance associated with the evolution of regional climate. Thus, changes in the physical nature of Hvítárvatn sediment reflect climate driven changes in ice cap aerial extent. Sediment accumulation rate, MS, density, and % silt + clay (%SC), are all expected to increase (decrease) with increasing (decreasing) glacial erosion (e.g. Leonard, 1997; Dahl et al., 2003 and references therein).

Following a brief period of high sedimentation rates directly above the basal Saksunarvatn tephra layer, sedimentation rates maintain a low average of ca 0.05 cm a^{-1} through the early Holocene, interrupted by a multi-centennial peak 8.5 to 8.0 ka. Sediment density, MS and %SC are elevated at the start of the record but decrease to minimal values by 9.0 ka, before increasing in concert with the peak in sedimentation rates after 8.5 ka. Low values of sediment density, MS, and %SC, accompany minimum sediment accumulation rates from 7.9 to 7.0 ka. All four physical proxies begin sustained increases at ~6 ka, with notable increases in density and MS at ca 5.5 ka, and strong increases in sedimentation rate at ca 4.2 and 3.0 ka. The sediment fill maintained a relatively high average bulk density of $2.0 \pm 0.1 \text{ g cm}^{-3}$ during the past 4 ka, with a prominent deviation to low density immediately above the H3 tephra layer; a similar negative deviation is also seen in the MS record. Sediment deposition rates increase dramatically in the 13th century AD, with two maxima at ca 1500 AD and ca 1935 AD that are

separated by a brief decline in the 16th century AD (Fig. 4). Maximum Holocene sedimentation rates are achieved during the 1935 AD peak, when average sediment deposition in core HVT03-1 is 2.5 cm a^{-1} . Significant IRD concentrations in the cores, which define the timing of Langjökull's maximum extension, are restricted to the late 18th and 19th centuries AD, and are coincident with the period of maximum sediment accumulation rates. The sudden decreases in sedimentation rates and IRD deposition shortly after 1940 AD are contemporaneous with the photographically documented retreat of the outlet glacier Suðurjökull from the lake.

4.3. Organic matter properties

Hvítárvatn sediments contain OM derived from a combination of aquatic and terrestrial (soil) sources, each with characteristic signatures that are independent of sedimentation rate (Larsen et al., 2011). The C:N and $\delta^{13}\text{C}$ of Holocene soil bulk OM in the lake catchment averages 13.6 ± 1.0 and -24.9 ± 0.6 , respectively ($n = 19$). These values represent the terrestrial end member of OM deposited in the lake and provide a reference for evaluating OM source contribution to the lake sediment. Proxy values indicative of terrestrial OM imply increased wind, glacier, and/or stream erosion of soil-covered terrain (Geirsdóttir et al., 2009a; Larsen et al., 2011).

Lake sediment $\text{TOC}_{\%}$ is initially low, increasing after 9.1 ka to average values until 3.5 ka. The extremely low OM concentrations

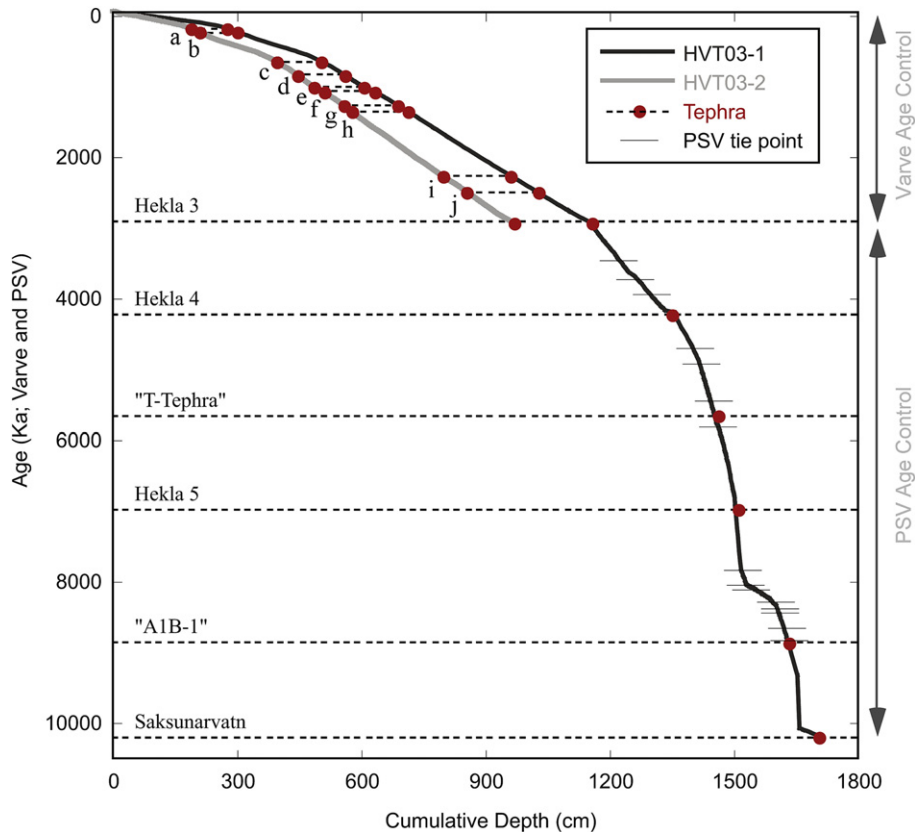


Fig. 3. Age model for cores HVT03-1 and HVT03-2 constructed by splicing the varve chronology for past ~3 ka (Larsen et al., 2011) with the PSV-derived chronology for older sediments (Ólafsdóttir, 2010). The positions of ten tephra layers (a–j) used to constrain the varve chronology are shown (see Larsen et al., 2011 for discussion) along with six labeled prehistoric tephra and PSV tie points used by Ólafsdóttir (2010).

at the start of the record precluded our ability to obtain accurate C:N and $\delta^{13}\text{C}$ analyses from 10.2 to 9.1 ka. Both TOC_Q and C:N experience a brief, strong peak at ca 8.2 ka. A broad TOC_Q maximum centered around 6.0 ka is followed by a trend of decreasing TOC_Q that is interrupted by large positive excursions at ca 4.8, 4.2, 3.0, 1.4, and 0.3 ka (Fig. 5). Organic matter concentrations are low and highly variable for the last 2 ka. Although the positive excursions in TOC_Q are associated with increases in C:N, the long-term trend in TOC_Q is broadly inverse to that of C:N. High C:N values in the early Holocene decrease rapidly to a multi-millennial period of consistently low values (mean = 6) between ca 7.9 and 4.2 ka. Following a shift toward higher values at 4.2 ka and a temporary increase at 3.0 ka, C:N steadily increases over the past 2.5 ka, reaching a peak in the early 20th century AD. TOC_Q is minimal in the early Holocene, experiences a brief positive excursion at ca 8.2 ka, and subsequently maintains a long-term trend of low but steadily increasing values from 7.9 to ca 4.2 ka. After 4.2 ka, TOC_Q becomes elevated and highly variable with prominent peaks at ca 3.0 ka and in the last millennium AD (Fig. 5).

Notable features of the $\delta^{13}\text{C}$ profile are the negative excursions at 8.5, 8.2 and 6.5 ka, and the lasting shift toward more depleted values at 4.2 ka. The highly oligotrophic nature of proglacial lakes such as Hvítárvatn would suggest that changes in $\delta^{13}\text{C}$ reflect variations in the proportion of terrestrial OM washing into the lake rather than changes in primary productivity or nutrient availability (e.g. Langdon et al., 2010). The strong decreases in $\delta^{13}\text{C}$ are associated with increasing C:N and TOC_Q , implying that sedimentary OM is dominated by terrestrial sources and that all three proxies are sensitive to landscape disturbances related to colder, windier conditions (Fig. 5). This scenario is also supported by the long-

term trends in $\delta^{13}\text{C}$ and C:N to values typical of regional soils (Fig. 5).

The timing of the above events, and particularly the 8.7 to 7.9 ka perturbation, is synchronous with major decreases in BSi, total diatom concentration, and %benthic diatoms (Db_Q ; Fig. 6). Similarities between these proxies are demonstrated by the strong correlation of diatom concentrations with BSi ($R^2 = 0.54$) and Db_Q ($R^2 = 0.53$) for the past 8 ka. All three proxies are high from 7.9 to 5.5 ka, decrease from 5.5 to 4.2 ka, and remain relatively low from 4.2 ka to present (Fig. 6). The composition of diatom communities at Hvítárvatn, including the relative abundance of planktonic and benthic species, is heavily influenced by nutrient and light availability associated with Langjökull activity (Black, 2008). Fluctuations in ice cap size and sediment delivery govern changes in water column turbidity and are recorded by the proportion of benthic diatoms to the total floral assemblage. High concentrations of volcanic glass in lake sediments can influence BSi measurements, and pure tephra layers from Hvítárvatn cores returned BSi concentrations of up to 4% (Black, 2008). However, the strong positive correlation of BSi to total diatom abundance and Db_Q indicates that BSi is a robust measure of lake productivity, although we emphasize relative trends in the BSi record rather than absolute values.

5. Climate and ice cap reconstruction

5.1. Holocene climate at Hvítárvatn and Langjökull development

Multiple physical and biological proxies at Hvítárvatn provide a record of environmental conditions and ice cap activity from

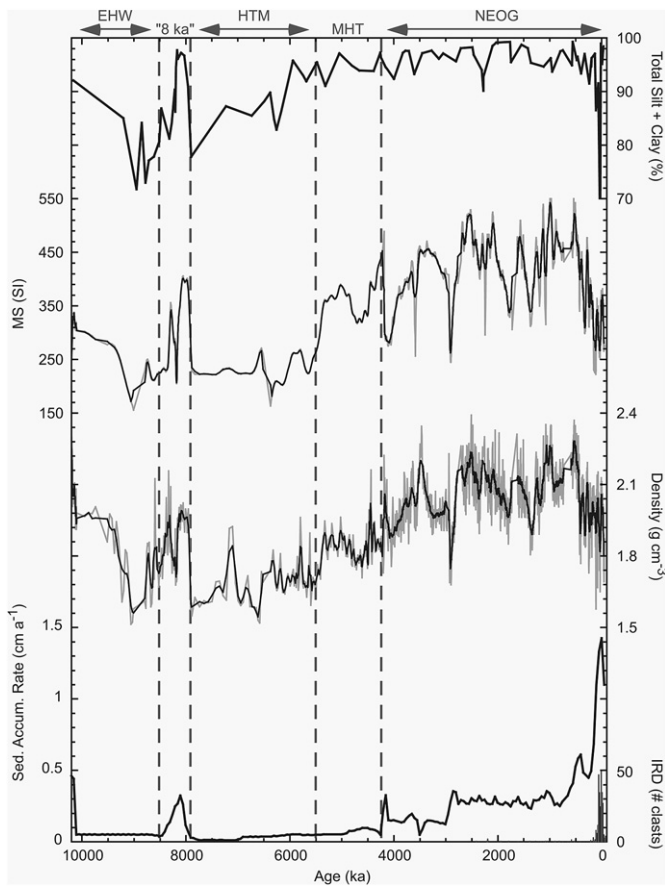


Fig. 4. Physical proxies contained in Hvítárvatn sediments. Bold lines represent approximately 50-year running averages superimposed on more highly resolved data shown behind in gray. Ice-rafted debris was counted in 20-year intervals in cores HVT03-1 and HVT03-2 and presented as an average number of clasts per 20-years.

central Iceland. In the discussion below, we present the Hvítárvatn record in the context of North Atlantic Holocene climate variability, placing an emphasis on intervals where prominent changes are seen in several proxies, and on comparisons to regional climate series. Because of the influence Langjökull exerts on downstream lake processes, the Holocene paleoenvironmental conditions at Hvítárvatn are reconstructed with a focus on ice cap development.

5.1.1. Early Holocene (10.2 to 8.7 ka): lake ontogeny and early warmth

The Hvítárvatn climate record begins following the uppermost Saksunarvatn tephra at the base of core HVT03-1. Although mounting evidence from this site (Black, 2008) and elsewhere (Wastl et al., 2001; Johannsdóttir et al., 2005; Lind et al., 2011) suggest that this widespread tephra layer may actually represent multiple closely-spaced eruptions of the Grímsvötn volcanic system rather than a single event, we assign the conventional age of 10.2 ka reported by Grönvold et al. (1995) to the base of our record. High sedimentation rates, elevated bulk density, and the laminated nature of the sediment for the century following the ~1.2 m tephra layer are indicative of an unstable, freshly deglaciated landscape coming into equilibrium with local climate. The basal sediment character may also reflect the waning influence of the main Iceland Ice Sheet as it retreated from the catchment. By this time, the regional equilibrium line altitude (ELA) was high enough that glacier ice in the location of present-day Langjökull would have melted completely.

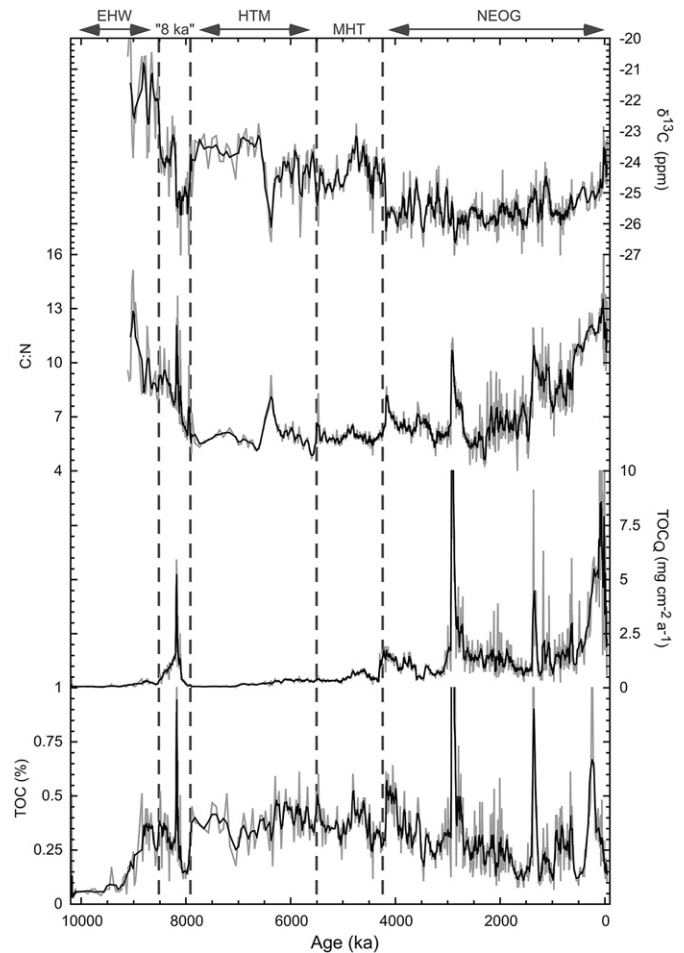


Fig. 5. Total organic carbon concentration (TOC_x), the mass flux of total organic carbon (TOC_Q), organic matter C:N, and $\delta^{13}\text{C}$ from core HVT03-1. Bold lines represent an approximately 50-year smoothing of data shown behind in gray.

High, but decreasing density, MS and %SC from 10.2 ka until 9.0 ka suggest increasing catchment stabilization following regional deglaciation, while gradually increasing TOC_x and BSi reflect increasing lake primary productivity in response to warm summers and biological immigration (Figs. 4–6). A portion of the signal during this period of flux may be associated with lake ontogeny related to catchment development and/or vegetation colonization. We interpret the low sedimentary OM values in the early Holocene to suggest at least 1 ka, and possibly longer, were required after deglaciation before the lake and catchment biota reached an equilibrium state.

Physical and biological proxies record a distinct warm interval from ca 9.0 to 8.7 ka. High diatom concentrations during this interval are composed almost exclusively of benthic species, suggesting both high productivity and clear water, requiring the absence of glacial erosion in the catchment. Elevated C:N values suggest contributions from developing regional soil (Figs. 5 and 6).

5.1.2. The 8 ka event (8.7 to 7.9 ka)

Early Holocene warmth is interrupted by two rapid shifts to cooler conditions at ca 8.5 and 8.2 ka. These perturbations have similar durations of ca 200 years, and are interpreted to represent two pulses of a major environmental perturbation between 8.7 and 7.9 that includes the well-documented “8 ka event” seen in many Northern Hemisphere climate records (e.g. Alley and Ágústsdóttir, 2005 and references therein). Low diatom concentrations, and

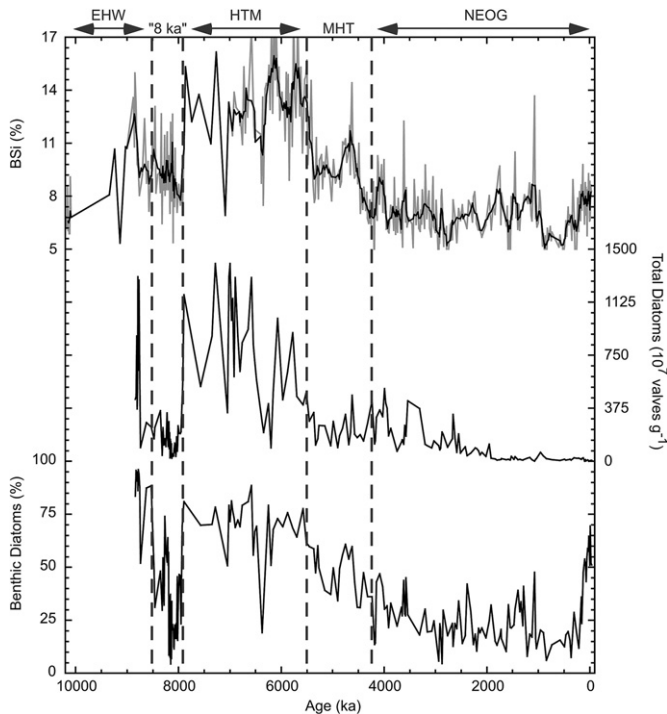


Fig. 6. Benthic diatom relative abundance, total diatom concentration, and biogenic silica (BSi) measured in core HVT03-1. Bold lines represent an approximately 50-year smoothing.

increasing sediment density and %SC after 8.7 ka, hint at progressively colder conditions (Figs. 4 and 6). At 8.5 ka, a >50% drop in benthic diatom concentrations and accompanying peaks in sediment density, MS and %SC point toward rapid increases in water turbidity and minerogenic deposition. Relatively high C:N and $\text{TOC}_{\%}$, along with a decrease in $\delta^{13}\text{C}$, suggest an increased contribution of soil to the lake. Further evidence for soil erosion comes from terrestrial stratigraphic sections excavated in the catchment. These sections commonly contain robust sequences of mid and late Holocene tephra, yet rarely predate Hekla 5 (~7 ka; Larsen and Thorarinsson, 1977) implying a period of landscape stripping prior to 7 ka. Together, the proxy data and empirical evidence reflect a substantial climate event that initiated landscape destabilization and/or glacier activity in the watershed. We interpret the behavior of the proxy data to be a function of soil erosion by deflation and alluviation, combined with the possible formation of glacial ice in the catchment, both indicating a shift toward colder summers in the highlands. The second cold pulse was initiated by 8.2 ka following an apparent reversal and/or brief (~100 years) return to mild conditions seen in all proxies. This more severe cold event lasted until 7.9 ka, and resulted in continued soil erosion and/or a second glacier advance. At its height, all proxies attained values comparable to those seen during the past millennium (Figs. 4–6). However, the absence of defined varves in the sediment fill, suggests that if present, this “proto”-Langjökull’s aerial extent was much smaller than during the late Holocene (Larsen et al., 2011) and that perennial ice was restricted to only the highest portions of the catchment; in agreement with the model simulation of Flowers et al. (2008).

5.1.3. Holocene thermal maximum (7.9 to 5.5 ka)

All proxy data reflect a sharp transition out of the 8 ka event and the shift to peak summer warmth by 7.9 ka (Figs. 4–6). The pronounced drops in sedimentation rate, density, MS and %SC

indicate less erosion and transport of minerogenic material to the lake, while the dominance of diatom assemblages by benthic species represents a large reduction in suspended sediment and greater light availability. Both lines of evidence suggest Langjökull was absent from the catchment. Low C:N, in conjunction with low TOC_{Q} and higher $\delta^{13}\text{C}$, reflects autogenic production and suggests a stable watershed with minimal soil erosion. The combined proxy data indicate that the shift back to warm conditions was not only swift but also enduring, with elevated summer temperatures lasting until ca 5.5 ka. Maximum BSi and diatom abundance during this time reflect high productivity. The combination of ice-free conditions, landscape stability, and warmer summers depict a relatively mild climate and define the HTM at Hvítárvatn between 7.9 and 5.5 ka. Although there is evidence for high summer temperatures in the early Holocene (5.1.1), we place the start of the HTM after the “8 ka event”, when all Hvítárvatn proxies indicate persistent, millennial-scale warmth.

The transition out of the HTM occurs in a stepped manner, beginning with a perturbation centered at 6.4 ka followed by a subsequent irreversible climate shift at ca 5.5 ka (Figs. 4–6). Proxy behaviors during the first perturbation are similar to the “8 ka event” and reflect a ~250-year cooling event that resulted in reduced lake productivity and landscape instability. However, a lack of change in sedimentation rates suggests that the duration or magnitude of inferred cooling was incapable of initiating substantial growth of Langjökull. Significant recovery from this event was achieved by 6.2 ka, with high BSi and $\text{Db}_{\%}$ suggesting a return to warm summers and stable landscapes (Fig. 6).

5.1.4. Mid Holocene transition (5.5 to 4.2 ka): the shift from warm to cold

The change in climate proxies at ca 5.5 ka marks the termination of HTM conditions and the advent of progressively cooler summers in the highlands that characterize the Neoglaciation. This shift is most clearly observed as a drop in BSi and diatom abundance, reflecting reduced productivity (Fig. 6). A step-wise increase in sediment density and MS, together with a decrease in benthic flora, indicates increased minerogenic input to the lake. A second cooling step at 4.2 ka is characterized by a large increase in sedimentation rate, preceded by the first appearance of varves, indicating a significant increase in glacier size (Fig. 4). At this same time, a step change in C:N, TOC_{Q} , $\delta^{13}\text{C}$, and BSi reflect colder summers and greater soil erosion (Figs. 5 and 6). The abrupt nature of these changes suggests a threshold-type response of Langjökull and catchment stability to increasingly colder summers. Stratigraphically, these variations occur immediately above the Hekla 4 tephra layer. Hekla 4 produced approximately 9 km^3 of ejected material (Larsen and Thorarinsson, 1977) and forms one of the thickest tephra layers in the sediment cores above the Saksunarvatn tephra. Regional impacts of the eruption and tephra deposition may have exacerbated the effects of the cooling trend that began ca 5.5 ka. We hypothesize that the Hekla 4 eruption initiated a brief period of decreased summer temperature and increased vegetation damage due to tephra abrasion, and that these perturbations resulted in an accelerated response of Langjökull and the watershed environment to the preconditioning effects of the longer-term cooling trend.

An evaluation of the proxy data during the transitional period from HTM warmth to Neoglacial cooling emphasizes the importance of having multiple independent climate indicators when reconstructing the evolution of paleoenvironments. Because proxies often respond preferentially to certain climate parameters, a suite of proxies provides a more robust interpretation of environmental change. For example, Hvítárvatn productivity indicators reflect abrupt summer cooling at 5.5 ka, while physical proxies

suggest a stepped decline into Neoglacial conditions, and sedimentary OM values do not show clear evidence for landscape instability until 4.2 ka (Figs. 4–6). Synthesizing the available data, we interpret the period from 5.5 to 4.2 ka as an interval of change, acknowledging that decreasing summer temperatures were impacting the catchment conditions by 5.5 ka, but asserting that major glacier and environmental responses, including significant ice expansion, were delayed until 4.2 ka. The lag in OM proxy reactions to Neoglacial cooling may reflect the time required for soil mobilization to occur in response to reduced vegetation cover within the catchment.

5.1.5. Neoglaciation (4.2 ka to present)

After the shift at 4.2 ka, the glacier and environmental proxies reflect a general cooling trend containing multiple abrupt variations in glacier activity and catchment stability. The continuously varved nature of the sediment after 4.2 ka indicates that Langjökull was present and contributing erosion products to the lake. High sediment density and MS reflect the increased minerogenic content, while elevated %SC and decreasing benthic diatom abundance require high suspended sediment loads (Figs. 4 and 6). The stepped pattern seen in many of these proxies suggest that the Neoglacial cooling may have occurred in discrete steps rather than as a monotonic trend. Subsequent to the expansion at 4.2 ka, proxy data imply periods of significant ice cap expansion at ca 2.9, 1.4 and 0.7 ka. The 2.9 ka advance is accompanied by a large increase in terrestrial OM inwash, indicating landscape instability, and has been associated with the eruption of Hekla 3 (Larsen et al., 2011). The relatively constant sediment accumulation rate during the ~1.5 ka following this event, suggests that Langjökull's aerial extent remained fairly uniform. The second two advances coincide with the Dark Ages Cold Period (DACP) and Little Ice Age (LIA), and are separated by 3 centuries of mild conditions corresponding to the Medieval Warm Period (MWP; Larsen et al., 2011). The start of the LIA is marked by a dramatic increase in varve thickness and C:N in the 13th Century (Figs. 4 and 5). Changes in sedimentation rate and other proxies, indicate that Langjökull advanced in two phases, reaching the lakeshore by ~1760 AD, and achieving its Holocene maximum ice stand in the 19th Century. Changes in environmental conditions and ice cap activity through the past 3 ka are discussed in detail in Larsen et al. (2011).

5.2. Non-linear Holocene climate change in Iceland

This study presents the first continuous, high-resolution record of Holocene climate from the interior highlands of Iceland. The Hvítárvatn sediments record a variable Holocene climate, distinguished by irregular fluctuations superimposed on a long-term trend of early summer warmth and subsequent shift toward cooler conditions. All proxies generally follow the gradual decline in Northern Hemisphere 60 °N summer insolation (Berger and Loutre, 1991, Fig. 7) indicating a coherent response to orbitally driven climate change for the last ~10 ka. However, the non-linear changes in the proxy data suggests both complex interactions in response to declining insolation, and the presence of additional forcing agents or strong feedbacks operating on varying timescales.

Although summers were already warm at the start of the record, peak warmth was delayed until after ~8 ka, lagging peak insolation by ~3 ka (Fig. 7). Delayed HTM summer warmth has been observed in other climate records in and around Iceland (Fig. 7), and has been attributed to altered ocean circulation on the West and Northwest Iceland shelf associated with meltwater from retreating Pleistocene ice sheets (Kaufman et al., 2004; Geirsdóttir et al., 2009b). The inferred absence of Langjökull, combined with catchment stability from 7.9 to 5.5 ka, reflects persistent summer warmth, interrupted

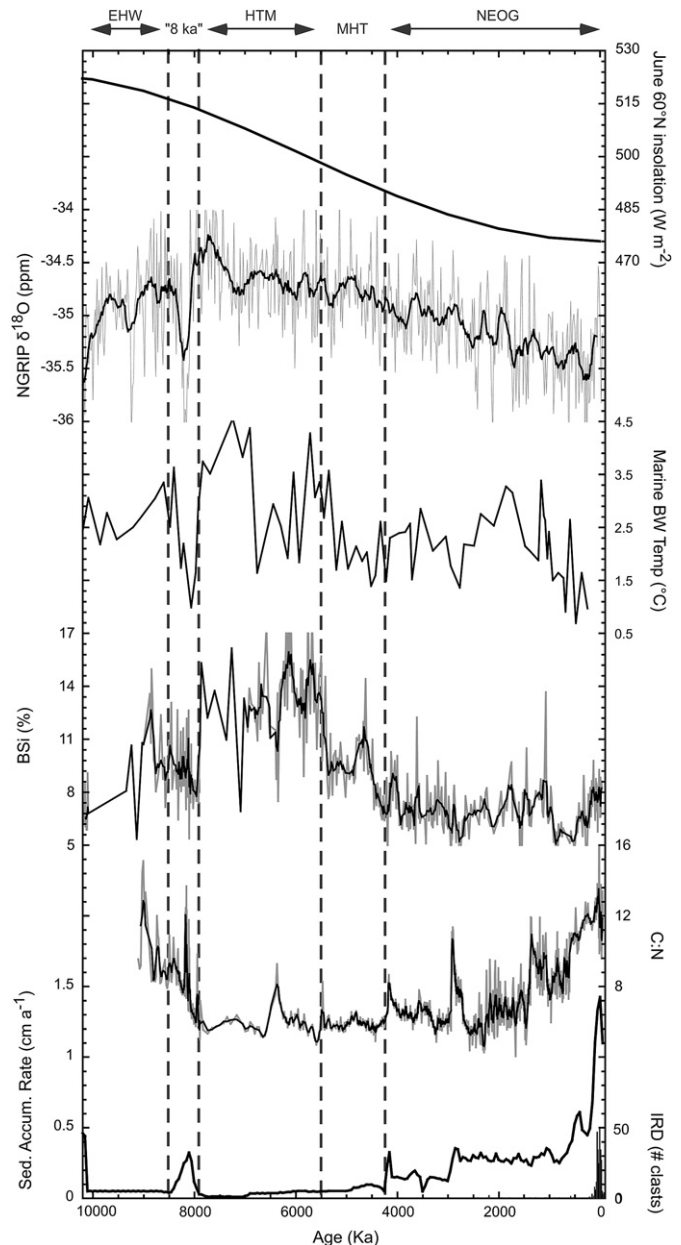


Fig. 7. Comparison of Hvítárvatn sedimentation rate, IRD, C:N and BSI, with selected North Atlantic climate records (NGRIP data from North Greenland Ice Core Project members, 2004; Vinther et al., 2006; NW Iceland fjord core MD99-2265 BWT data from Ólafsdóttir, 2010) and 60 °N summer insolation (Berger and Loutre, 1991).

only by a brief but significant perturbation around 6.4 ka. Model simulations of Langjökull, driven by Greenland isotope-derived temperature data and constrained with empirical evidence from Hvítárvatn, suggest that an ice-free HTM requires mean summer temperatures ~3 °C above present (Flowers et al., 2008; 1961–1990 AD reference period). The delayed onset and estimated magnitude of HTM warmth at Hvítárvatn stands in agreement with chironomid based reconstructions from northern Iceland that reflect HTM July temperatures of approximately 2–2.5 °C above present (Caseldine et al., 2006). Paleoclimatological studies describe a trend of progressively strengthening Atlantic water circulation through the early Holocene that resulted in increasing SSTs (e.g. Eiríksson et al., 2000a; Castañeda et al., 2004; Smith et al., 2005; Knudsen et al., 2008; Ólafsdóttir et al., 2010) with an apparent latitudinal gradient in timing and magnitude (Andersen

et al., 2004). Surface and bottom water temperatures on the North Iceland Shelf reached maximum warmth immediately following the 8 ka cold event (Castañeda et al., 2004; Knudsen et al., 2008; Ólafsdóttir, 2010), a finding comparable to Hvítárvatn, suggesting that terrestrial and marine environments are responding to the same large-scale evolution of North Atlantic circulation patterns.

The stepped transition from HTM to Neoglaciation in the central highlands beginning at 5.5 ka suggests a disproportionate environmental response to continuously decreasing summer insolation, and is likely associated with a restructuring of atmospheric and/or oceanic circulation (e.g. Alley et al., 1999; Andersen et al., 2004). A persistent trend toward colder ocean temperatures around Iceland beginning by ~6 ka is seen in marine sediment core proxies (e.g. Eiríksson et al., 2000a; Andersen et al., 2004; Castañeda et al., 2004; Smith et al., 2005; Bendle and Rosell-Melé, 2007), but is not reflected in chironomid-derived summer temperature reconstructions from lakes in North Iceland (Caseldine et al., 2003; Axford et al., 2007). Many of the subsequent Neoglacial cooling events (4.2, 2.9, 1.4, and 0.7 ka) that resulted in Langjökull advance and/or catchment instability are also detected in marine archives (e.g. Eiríksson et al., 2000b; Castañeda et al., 2004; Bendle and Rosell-Melé, 2007; Ólafsdóttir et al., 2010). These step-change events are consistent with coordinated changes in multiple proxies from the non-glacial lake Haukadalsvatn in western Iceland (Geirsdóttir et al., 2009a) and from terrestrial records in the British Isles (Charman, 2010 and references therein). The final, most extreme cooling at 0.7 ka (~1250 AD) marks the LIA onset, and resulted in intensive landscape destabilization and the maximum Holocene stand of Langjökull (Fig. 7). The ELA lowering during peak LIA conditions implies a ~1 °C temperature decrease relative to present, suggesting a total Holocene temperature change of 4 °C, from peak HTM to peak LIA summer conditions (Flowers et al., 2007).

An important discrepancy between the glacier record presented here and some earlier moraine studies centers around the maximum extent of Neoglacial advances across Iceland. The physical and organic matter proxy data from Hvítárvatn clearly show that Langjökull's LIA advance was by far the largest glacial advance in at least the last 8 ka. This stands in direct contrast to studies that have reported Neoglacial advances of valley and/or mountain glaciers to regions outside of their LIA limits (e.g. Stötter et al., 1999 and references therein; Kirkbride and Dugmore, 2006; Principato, 2008). Two lines of evidence have been used to infer extensive early Neoglacial advances. Some moraines situated a short distance distal to a LIA moraine are mantled by tephra-bearing soils, in which the oldest tephra are between 1 and 5 ka old. The oldest tephra is sometimes interpreted to be a close limiting minimum age for the underlying moraine. However, the lack of older Holocene tephra can be explained by widespread eolian erosion. For example, stratigraphic sections in the Hvítárvatn catchment commonly contain interbedded tephra only of middle Holocene and younger ages, yet directly overlie till deposited during regional deglaciation, ~10.2 ka. A second line of evidence is derived from stratigraphic sections in which unsorted bouldery units are bracketed by middle Holocene tephra. The bouldery units are inferred to represent buried moraines, but evidence that the thin stony layers represent primary constructional moraines is equivocal and open to interpretation. We suggest that such exposures be interpreted cautiously. It is unlikely that the early Neoglacial advances of any non-surging glacier in Iceland were significantly larger than their LIA maxima.

The most remarkable features of the Hvítárvatn multi-proxy record are the abrupt and large-scale climate changes observed at ~8.7–7.9, 6.4, 5.5, 4.2, 2.9, 1.4, and 0.7 ka (Fig. 7). Each event is associated with increased glacier activity and/or catchment

instability, reflecting significant regional summer cooling, and their timing is consistent with observed periods of hemispherically-coherent rapid climate change involving bipolar cooling and the reorganization of atmospheric and oceanic circulation (Bond et al., 2001; Mayewski et al., 2004 and references therein). With the important exception of the 8 ka event, the most plausible forcing mechanisms are solar variability and volcanic emissions superimposed on long-term insolation changes (Mayewski et al., 2004). Northern Hemisphere climate anomalies associated with the 8 ka event have been attributed to changes in North Atlantic overturning circulation from the catastrophic drainage of ice-marginal lake water through the Hudson Strait ~8.47 ka (Barber et al., 1999). Typically identified in Greenland Ice Sheet proxies as a short lived (100–200 years) cold reversal of early Holocene warming, this event is expressed as a broader interval (500–600 years) of decreased water temperature on the North Iceland Shelf, with marine core proxies reflecting 1–3 °C cooling (Fig. 7; Knudsen et al., 2004; Bendle and Rosell-Melé, 2007; Ólafsdóttir, 2010). At Hvítárvatn, two distinct and severe cold pulses at ca 8.5 and 8.2 ka represent the culmination of a gradual cooling trend beginning ~8.7 ka (Figs. 4–6). The longer duration of suppressed temperatures found here and elsewhere in Iceland (Geirsdóttir et al., 2009b and references therein) invokes additional trigger mechanisms, such as increased volcanism, and reflects a dynamical response of terrestrial environments in the North Atlantic to changing ocean and atmosphere boundary conditions on which the 8 ka cold excursion is superimposed. The subsequent cooling shifts at Hvítárvatn, including those at 4.2 ka and later (Larsen et al., 2011; Miller et al., 2012), have been related to both local perturbations and more remote forcing mechanisms, such as solar variability and global volcanism.

The non-linear changes presented here constitute some of the most coherent terrestrial evidence from Iceland for widespread, quasi-periodic Holocene climate shifts (e.g. Denton and Karlén, 1973). We emphasize these events in the Hvítárvatn record to highlight the glacier and environmental response to various forcing mechanisms and related climate feedbacks, and to draw attention to the strong connection between terrestrial and marine environments of the North Atlantic.

6. Conclusions

Multiple physical and organic matter proxies preserved in securely dated Hvítárvatn sediments provide a continuous record of Holocene environmental conditions and ice cap evolution in central Iceland at unprecedented age resolution. Proxy data indicate that, following regional deglaciation of the main Iceland ice sheet by 10.2 ka, glacier ice was absent from the catchment during early Holocene warmth. This early, insolation driven warmth was interrupted between 8.7 and 7.9 ka by two pulses of abrupt cooling that initiated catchment instability and/or the formation and brief expansion of Langjökull. Subsequent ice-free and mild conditions persisted from ca 7.9 to 5.5 ka, representing the HTM in central Iceland. During this time, proxy data, including diatom abundance and composition, reflect increased within-lake primary productivity, a clear water column, and stable conditions of the surrounding watershed. The transition out of the HTM occurred as a step-wise shift toward Neoglaciation after ca 5.5 ka that included Langjökull growth and catchment destabilization, which was accelerated at ca 4.2 ka, with increasingly cold and variable conditions persisting through the late Holocene. Once established in the watershed, Langjökull remained present, dominating the abiotic and biotic components of the lacustrine system, primarily through meltwater discharge of minerogenic erosion products. The climate of the past two millennia is characterized by two significant

periods of landscape instability and glacial activity beginning in the 6th and 13th centuries AD, that correspond to the DACP and LIA, and that are separated by a relatively stable interval in Medieval times. Langjökull reached its Holocene maximum dimensions in the 19th century AD when soil erosion in the highlands was greatest.

This study presents the first continuous record of ice cap extent for the entire Holocene and clearly demonstrates that the LIA contained the most extensive glacial advance of the Neoglacial interval. The strong multi-proxy signal at Hvítarvatn implies that the LIA was the coldest period of the last 8 ka and suggests that is unlikely for any non-surgingly Iceland glacier to have reached dimensions significantly larger than its LIA maximum at any time during the Holocene. Additional multi-proxy evidence for abrupt and step-wise cooling events at ~8.7–7.9, 6.4, 5.5, 4.2, 2.9, 1.4, and 0.7 ka reflect a complex Holocene climate with recurring non-linear changes that resulted in landscape instability and glacier advances in central Iceland.

Acknowledgments

Sediment cores were obtained using the DOSECC GLAD-200 coring system with financial support from the US National Science Foundation (OPP-0138010) and the Icelandic Centre of Research, RANNIS (#040233021). Additional support was provided by the Icelandic fund for graduate students, grant #R09031/5264, and by the VAST (Volcanism in the Arctic System) Project, through NSF-OPP-ARC 0714074 and RANNIS #0070272011. Thanks to Thorsteinn Jónsson, Sveinbjörn Steinthórsson, and Doug Schnurrenberger for their great work in the field, and to the people at the LRC, University of Minnesota, for laboratory assistance. This manuscript was improved by comments from two anonymous reviewers.

References

- Alley, R.B., Ágústsdóttir, A.M., 2005. The 8k event: cause and consequences of a major Holocene abrupt climate change. *Quaternary Science Reviews* 24, 1123–1149.
- Alley, R.B., Ágústsdóttir, M., Fawcett, P.J., 1999. Ice-core evidence of Late Holocene reduction in North Atlantic Ocean heat transport. In: Clark, P.U., Webb, R.S., Keigwin, L.D. (Eds.), *Mechanisms of Global Climate Change at Millennial Time Scales*. Geophys. Monogr. Ser. vol. 112. AGU, Washington, D. C. pp. 301–312.
- Andersen, C., Koc, N., Jennings, A., Andrews, J.T., 2004. Nonuniform response of the major surface currents in the Nordic Seas to insolation forcing: implications for the Holocene climate variability. *Paleoceanography* 19, PA2003. doi:10.1029/2002PA000873.
- Axford, Y., Miller, G.H., Geirsdóttir, Á., Langdon, P.G., 2007. Holocene temperature history of northern Iceland inferred from subfossil midges. *Quaternary Science Reviews* 26, 3344–3358.
- Axford, Y., Geirsdóttir, Á., Miller, G.H., Langdon, P.G., 2009. Climate of the little ice age and the past 2000 years in northeast Iceland inferred from chironomids and other lake sediment proxies. *Journal of Paleolimnology* 41, 7–24.
- Barber, D.C., Dyke, A., Hillaire-Marcel, C., Jennings, A.E., Andrews, J.T., Kerwin, M.W., Bilodeau, G., McNeely, R., Southon, J., Morehead, M.D., Gagnon, J.M., 1999. Forcing of the cold event of 8,200 years ago by catastrophic drainage of Laurentide lakes. *Nature* 400, 344–348.
- Bendle, J.A.P., Rosell-Melé, A., 2007. High-resolution alkenone sea surface temperature variability on the north Icelandic shelf: implications for Nordic Seas palaeoclimatic development during the Holocene. *Holocene* 17, 9–24.
- Berger, A., Loutre, M.F., 1991. Insolation values for the climate of the last 10,000,000 years. *Quaternary Science Reviews* 10, 297–317.
- Black, J., 2008. Holocene climate change in south central Iceland: a multiproxy lacustrine record from glacial lake Hvítarvatn. Ph.D. thesis, University of Colorado, Boulder.
- Black, J., Miller, G.H., Geirsdóttir, Á., Manley, W., Björnsson, H., 2004. Sediment thickness and Holocene erosion rates derived from a seismic survey of Hvítarvatn, central Iceland. *Jökull* 54, 37–56.
- Bond, G., Kromer, B., Beer, J., Muscheler, R., Evans, M.N., Showers, W., Hoffmann, S., Lotti-Bond, R., Hajdas, I., Bonani, G., 2001. Persistent solar influence on North Atlantic climate during the Holocene. *Science* 294, 2130–2136.
- Caseldine, C., Geirsdóttir, Á., Langdon, P., 2003. Efstadalsvatn—a multi-proxy study of a Holocene lacustrine sequence from NW Iceland. *Journal of Paleolimnology* 30, 55–73.
- Caseldine, C., Langdon, P., Holmes, N., 2006. Early Holocene climate variability and the timing and extent of the Holocene thermal maximum (HTM) in northern Iceland. *Quaternary Science Reviews* 25, 2314–2331.
- Castañeda, I.S., Smith, L.M., Kristjánsson, G.B., Andrews, J.T., 2004. Temporal changes in Holocene $\delta^{18}O$ records from the northwest and central north Iceland shelf. *Journal of Quaternary Science* 19, 321–334.
- Charman, D.J., 2010. Centennial climate variability in the British Isles during the mid-late Holocene. *Quaternary Science Reviews* 29, 1539–1554.
- Conley, D.J., Schelske, C.L., 2002. Tracking environmental change using lake sediments terrestrial, algal, and siliceous indicators. In: Smol, J.P., Birks, H.J.B., Last, W.M., Bradley, R.S., Alverson, K. (Eds.), *Developments in Paleoenvironmental Research*. Springer, Netherlands, pp. 281–293.
- Dahl, S.O., Bakke, J., Øyvind, L., Nesje, A., 2003. Reconstruction of former glacier equilibrium-line altitudes based on proglacial sites: an evaluation of approaches and selection of sites. *Quaternary Science Reviews* 22, 275–287.
- Denton, G.H., Broecker, W.S., 2008. Wobbly ocean conveyor circulation during the Holocene? *Quaternary Science Reviews* 27, 1939–1950.
- Denton, G.H., Karlén, W., 1973. Holocene climatic variations – their pattern and possible cause. *Quaternary Research*, 155–205.
- Desloges, J.R., 1994. Varve deposition and the sediment yield record at three small lakes of the Southern Canadian Cordillera. *Arctic and Alpine Research* 26 (2), 130–140.
- Dugmore, A.J., Cook, G.T., Shore, J.S., Newton, A.J., Edwards, K.J., Larsen, G., 1995. Radiocarbon dating tephra layers in Britain and Iceland. *Radiocarbon* 37, 379–388.
- Eiríksson, J., Knudsen, K.L., Haflidason, H., Henriksen, P., 2000a. Late-glacial and Holocene palaeoceanography of the north Icelandic shelf. *Journal of Quaternary Science* 15, 23–42.
- Eiríksson, J., Knudsen, K.L., Haflidason, H., Heinemeier, J., 2000b. Chronology of late Holocene climatic events in the northern North Atlantic based on AMS C-14 dates and tephra markers from the volcano Hekla, Iceland. *Journal of Quaternary Science* 15, 573–580.
- Flowers, G.E., Björnsson, H., Geirsdóttir, Á., Miller, G.H., Clarke, G.K.C., 2007. Glacier fluctuation and inferred climatology of Langjökull ice cap through the little ice age. *Quaternary Science Reviews* 26, 2337–2353.
- Flowers, G.E., Björnsson, H., Geirsdóttir, Á., Miller, G.H., Black, J.L., Clarke, G.K.C., 2008. Holocene climate conditions and glacier variation in central Iceland from physical modeling and empirical evidence. *Quaternary Science Reviews* 27, 797–813.
- Geirsdóttir, Á., Miller, G.H., Wattrus, N.J., Björnsson, H., Thors, K., 2008. Stabilization of glaciers terminating in closed water bodies: evidence and broader implications. *Geophysical Research Letters* 35, 1–5.
- Geirsdóttir, Á., Miller, G.H., Thordarson, T., Olafsdóttir, K.B., 2009a. A 2000 year record of climate variations reconstructed from Haukadalsvatn, West Iceland. *Journal of Paleolimnology* 41, 95–115.
- Geirsdóttir, Á., Miller, G.H., Axford, Y., Olafsdóttir, S., 2009b. Holocene and latest Pleistocene climate and glacier fluctuations in Iceland. *Quaternary Science Reviews* 28, 2107–2118.
- Glew, J.R., 1991. Miniature gravity corer for recovering short sediment cores. *Journal of Paleolimnology* 5, 285–287.
- Grönvold, K., Oskarsson, N., Johnsen, S.J., Clausen, H.B., Hammer, C.U., Bond, G., Bard, E., 1995. Ash layers from Iceland in the Greenland GRIP ice core correlated with oceanic and land sediments. *Earth and Planetary Science Letters* 135, 149–155.
- Gudmundsson, H.J., 1997. A review of the Holocene environmental history of Iceland. *Quaternary Science Reviews* 16, 81–92.
- Hallsdóttir, M., 1991. Studies in vegetational history of north Iceland: a radiocarbon-dated pollen diagram from Flateyjar-dalur. *Jökull* 40, 67–81.
- Hallsdóttir, M., 1995. On the pre-settlement history of Icelandic vegetation. *Buvísindi* 9, 17–29.
- Hallsdóttir, M., Caseldine, C.J., 2005. The Holocene vegetation history of Iceland, state-of-the-art and future research. In: Caseldine, C., Russell, A., Harjardóttir, J., Knudsen (Eds.), *Iceland: Modern Processes and Past Environments*. Elsevier, Amsterdam, pp. 319–334.
- Hannesdóttir, H., 2006. Reconstructing environmental change in south Iceland during the last 12,000 years based on sedimentological and seismostratigraphical studies in lake Hestvatn. M.S. thesis, University of Iceland, Reykjavík.
- Jagan, A., 2010. Tephra stratigraphy and geochemistry from three Icelandic lake cores: a new method for determining source volcano of tephra layers. M.S. thesis, The University of Edinburgh.
- Jóhannsdóttir, G.E., 2007. Mid-Holocene to late glacial tephrochronology in west Iceland as revealed in three lacustrine environments. M.S. thesis, University of Iceland, Reykjavík.
- Jóhannsdóttir, G.E., Thordarson, T., Geirsdóttir, Á., Larsen, G., 2005. The widespread 10 ka saksunarvatn tephra: a product of three large basaltic phreatoplina eruptions? *European Geosciences Union, Geophysical Research Abstracts* 7, 05991.
- Karlén, W., 1981. Lacustrine sediment studies: a technique to obtain a continuous record of Holocene glacier variations. *Geografiska Annaler* 63, 273–281.
- Kaufman, D.S., Ager, T.A., Anderson, N.J., Anderson, P.M., Andrews, J.T., Bartlein, P.J., Brubaker, L.B., Coats, L.L., Cwynar, L.C., Duvall, M.L., Dyke, A.S., Edwards, M.E., Eisner, W.R., Gajewski, K., Geirsdóttir, A., Hu, F.S., Jennings, A.E., Kaplan, M.R., Kerwin, M.N., Lozhkin, A.V., MacDonald, G.M., Miller, G.H., Mock, C.J., Oswald, W.W., Otto-Bliesner, B.L., Porinchu, D.F., Ruhland, K., Smol, J.P., Steig, E.J., Wolfe, B.B., 2004. Holocene thermal maximum in the western Arctic (0–1801 W). *Quaternary Science Reviews* 23, 529–560.

- Kirkbride, M.P., Dugmore, A.J., 2001. Timing and significance of mid-Holocene glacier advances in northern and central Iceland. *Journal of Quaternary Science* 16, 145–153.
- Kirkbride, M.P., Dugmore, A.J., 2006. Responses of mountain lee caps in central Iceland to Holocene climate change. *Quaternary Science Reviews* 25, 1692–1707.
- Knudsen, K.L., Eiriksson, J., 2002. Application of tephrochronology to the timing and correlation of palaeoceanographic events recorded in Holocene and Late Glacial shelf sediments off north Iceland. *Marine Geology* 191, 165–188.
- Knudsen, K.L., Jiang, H., Jansen, E., Eiriksson, J., Heinemeier, J., Seidenkrantz, M.S., 2004. Environmental changes of north Iceland during the deglaciation of the Holocene: foraminifera, diatoms and stable isotopes. *Marine Micropaleontology* 50, 273–305.
- Knudsen, K.L., Søndergaard, M.K.B., Eiriksson, J., Jiang, H., 2008. Holocene thermal maximum off north Iceland: evidence from benthic and planktonic foraminifera in the 8600–5200 cal year BP time slice. *Marine Micropaleontology* 67, 120–142.
- Kristjansdóttir, G.B., Stoner, J.S., Jennings, A.E., Andrews, J.T., Grönvold, K., 2007. Geochemistry of Holocene cryptotephra from the north Iceland shelf (MD99-2269): intercalibration with radiocarbon and paleomagnetic chronostratigraphies. *Holocene* 17, 155–176.
- Langdon, P.G., Leng, M.J., Holmes, M., Caseldine, C.J., 2010. Lacustrine evidence of early-Holocene environmental change in northern Iceland: a multiproxy paleoecology and stable isotope study. *The Holocene* 20, 205–214.
- Larsen, G., Thórarinnsson, S., 1977. H4 and other acid Hekla layers. *Jökull* 27, 29–46.
- Larsen, D.J., Miller, G.H., Geirsdóttir, Á., Thordarson, T., 2011. A 3000-year varved record of glacier activity and climate change from the proglacial lake Hvítarvatn. *Quaternary Science Reviews* 30, 2715–2731.
- Leonard, E.M., 1997. The relationship between glacial activity and sediment production: evidence from a 4450-year varve record of neoglaciation in Hector Lake, Alberta, Canada. *Journal of Paleolimnology* 17, 319–330.
- Lind, E., Wastegard, S., Pearce, N., Lillja, C., 2011. Trace element chemistry of the saksunarvatn ash from the Faroe Islands – better chronological resolution? *International Union for Quaternary Research. Abstract* 3409.
- Massé, G., Rowland, S.J., Sicre, M., Jacob, J., Jansen, E., Belt, S.T., 2008. Abrupt climate changes for Iceland during the last millennium: evidence from high resolution sea ice reconstructions. *Earth and Planetary Science Letters* 269, 565–569.
- Mayewski, P.A., Rohling, E.E., Stager, J.C., Karlen, W., Maasch, K.A., Meeker, L.D., Meyerson, E.A., Gasse, F., van Kreveld, S., Holmgren, K., Lee-Thorp, J., Rosqvist, G., Rack, F., Staubwasser, M., Schneider, R.R., Steig, E.J., 2004. Holocene climate variability. *Quaternary Research* 62, 243–255.
- Meyers, P.A., Teranes, J.L., 2001. Sediment organic matter. In: Last, W.M., Smol, J.P. (Eds.), *Tracking Environmental Change Using Lake Sediments. Physical and Geochemical Methods*, vol. 2. Kluwer, Dordrecht, pp. 239–269.
- Miller, G.H., Geirsdóttir, Á., Zhong, Y., Larsen, D.J., Otto-Bliesner, B.L., Holland, M.M., Bailey, B.A., Refsnider, K.A., Lehman, S.J., Southon, J.R., Anderson, C., Björnsson, H., Thordarson, T., 2012. Abrupt onset of the little ice age triggered by volcanism and sustained by sea-ice/ocean feedbacks. *Geophysical Research Letters* 39, L02708. doi:10.1029/2011GL050168.
- Mortlock, R.A., Froelich, P.N., 1989. A simple method for the rapid determination of biogenic opal in pelagic marine sediments. *Deep-Sea Research Part A* 36, 1415–1426.
- North Greenland Ice Core Project members, 2004. High-resolution record of northern hemisphere climate extending into the last interglacial period. *Nature* 431, 147–151.
- Ólafsdóttir, S., 2010. Holocene marine and lacustrine paleoclimate and paleomagnetic records from Iceland: land-sea correlations. Ph.D. thesis, University of Iceland.
- Ólafsdóttir, S., Jennings, A.E., Geirsdóttir, Á., Andrews, J.T., Miller, G.H., 2010. Holocene variability of the North Atlantic Irminger current on the south and northwest shelf of Iceland. *Marine Micropaleontology* 77, 101–118.
- Oppo, D.W., McManus, J.F., Cullen, J.L., 2003. Palaeo-oceanography: deepwater variability in the Holocene epoch. *Nature* 422, 277–278.
- Paillard, D., Labeyrie, L., Yiou, P., 1996. Macintosh program performs time-series analysis. *Eos Transactions American Geophysical Union* 77, 379.
- Palmer, S., Shepherd, A., Björnsson, H., Pálsson, F., 2009. Ice velocity measurements of Langjökull, Iceland, from interferometric synthetic aperture radar (InSAR). *Journal of Glaciology* 55, 834–838.
- Pálsson, S., Vigfússon, G.H., 1996. *Gagnasafn aurburðarmælinga 1963–1995*. Orkustofnun, OS-96032/VOD-05 B, 270 pp. (in Icelandic).
- Principato, S., 2008. Geomorphic evidence for Holocene glacial advances and sea-level fluctuations on eastern Vestfirðir, northwest Iceland. *Boreas* 37, 132–145.
- Rundgren, M., 1998. Early Holocene vegetation of northern Iceland: pollen and plant macrofossil evidence from the Skagi peninsula. *The Holocene* 8, 553–564.
- Sicre, M.A., Yiou, P., Eiriksson, J., Ezat, U., Guimbert, E., Dahhaoui, I., Knudsen, K.L., Jansen, E., Turon, J.L., 2008. A 4500-year reconstruction of sea surface temperature variability at decadal time-scales off north Iceland. *Quaternary Science Reviews* 27, 2041–2047.
- Smith, L.M., Andrews, J.T., Castaneda, I.S., Kristjansdóttir, G.B., Jennings, A.E., Sveinbjörnsdóttir, A.E., 2005. Temperature reconstructions for SW and N Iceland waters over the last 10 cal ka based on delta O-18 records from planktic and benthic foraminifera. *Quaternary Science Reviews* 24, 1723–1740.
- Stoner, J.S., Jennings, A.E., Kristjansdóttir, G.B., Dunhill, G., 2007. A paleomagnetic approach toward refining Holocene radiocarbon-based chronologies: paleoceanographic records from the north Iceland (MD99-2269) and east Greenland (MD99-2322) margins. *Paleoceanography* 22, PA1209. doi:10.1029/2006PA001285.
- Stötter, J., Wastl, M., Caseldine, C., Haberle, T., 1999. Holocene palaeoclimatic reconstruction in northern Iceland: approaches and results. *Quaternary Science Reviews* 18, 457–474.
- Tómasson, H., 1993. Jökulstíflud vötn á Kili og hamfarahlaup í Hvítá í Árnessyslu. *Náttúrufræðingurinn* 62, 77–98.
- Vinther, B.M., Clausen, H.B., Johnsen, S.J., Rasmussen, S.O., Andersen, K.K., Buchardt, S.L., Seierstad, I.K., Siggaard-Andersen, M.-L., Steffensen, J.P., Svensson, A.M., Olsen, J., Heinemeier, J., 2006. A synchronized dating of three Greenland ice cores throughout the Holocene. *Journal of Geophysical Research* 111, D13102.
- Wastl, M., Stötter, J., 2005. Holocene glacier history. In: Caseldine, C., Russell, A., Harjardóttir, J., Knudsen, Ö. (Eds.), *Iceland: Modern Processes and Past Environments*. Elsevier, Amsterdam, pp. 221–240.
- Wastl, M., Stötter, J., Caseldine, C., 2001. Reconstruction of Holocene variations of the upper limit of tree or shrub birch growth in northern Iceland based on evidence from Vesturardalur-Skjádalur, Trollaskagi. *Arctic Antarctic and Alpine Research* 33, 191–203.